Cell Host & Microbe, Volume *29*

Supplemental Information

Induction of alarmin S100A8/A9 mediates activation of aberrant neutrophils in the pathogenesis of COVID-19

Qirui Guo, Yingchi Zhao, Junhong Li, Jiangning Liu, Xiuhong Yang, Xuefei Guo, Ming Kuang, Huawei Xia, Zeming Zhang, Lili Cao, Yujie Luo, Linlin Bao, Xiao Wang, Xuemei Wei, Wei Deng, Nan Wang, Luoying Chen, Jingxuan Chen, Hua Zhu, Ran Gao, Chuan Qin, Xiangxi Wang, and Fuping You

Supplemental Information

Figure S1. Antiviral innate immune disorder in the early stage of SARS-CoV-2 infection. (Related to Figure 1)

Figure S2. Analysis of the differences between coronavirus and influenza a virus infection. (Related to Figure 2)

Figure S3. Analysis of immune characteristics of mouse coronavirus MHV-A59 infection. (Related to Figure 2)

Figure S4. Aberrant neutrophils are closely associated with fatal coronavirus infection. (Related to Figure 3)

Figure S5. Analysis of the efficacy of Paquinimod in rescuing mice infected with coronavirus. (Related to Figure 4)

Figure S6. An attempt to treat mice infected with coronavirus via Azeliragon. (Related to Figure 5)

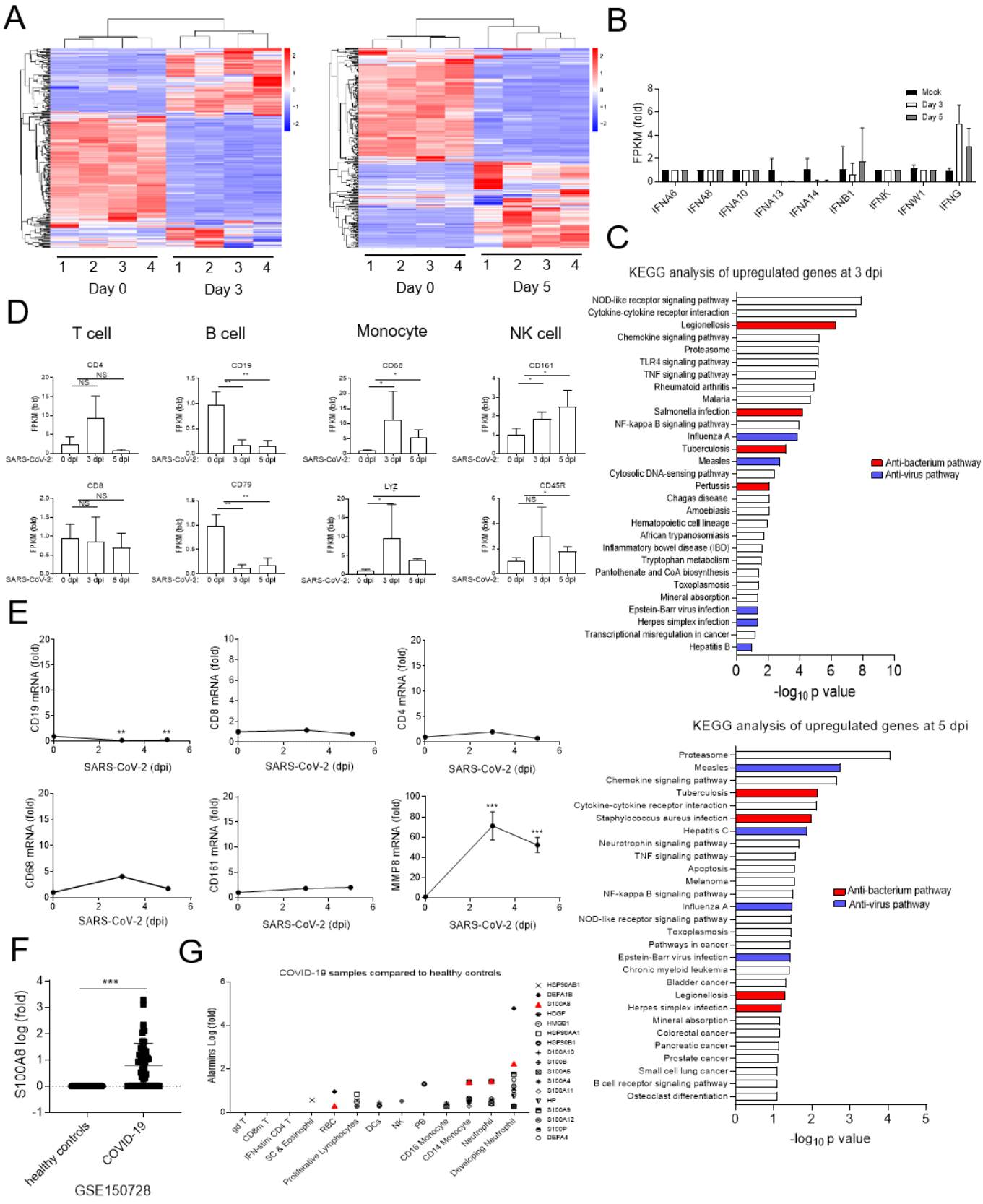

Figure S1. Antiviral innate immune disorder in the early stage of SARS-CoV-2 infection. (Related to Figure 1)

(A) Heat map depicting the differentially expressed genes in the lungs of rhesus macaques infected with SARS-CoV-2 at 3 dpi and 5 dpi. **(B)** The expression of IFNs was analyzed in the lungs of rhesus macaques infected with SARS-CoV-2 at 3 dpi and 5 dpi. **(C)** KEGG analysis of the differences in rhesus macaques infected with SARS-CoV-2 compared with Mock. **(D)** The expression of indicated marker genes was analyzed.

n = 4. **(E)** qRT-PCR analysis of indicated marker genes in the lungs of SARS-CoV-2-infected rhesus macaques at 0 dpi, 3 dpi and 5 dpi. *n=3*. **(F)-(G)** Analysis of *S100A8* (F) and alarmins (G) expression in peripheral blood from healthy control and COVID-19 patients. Fold change (FC) to healthy control (log10). Data from the peripheral blood of COVID-19 patients and healthy control correspond to GEO: GSE150728. (*P < 0.05; **P < 0.01; ***P < 0.001).

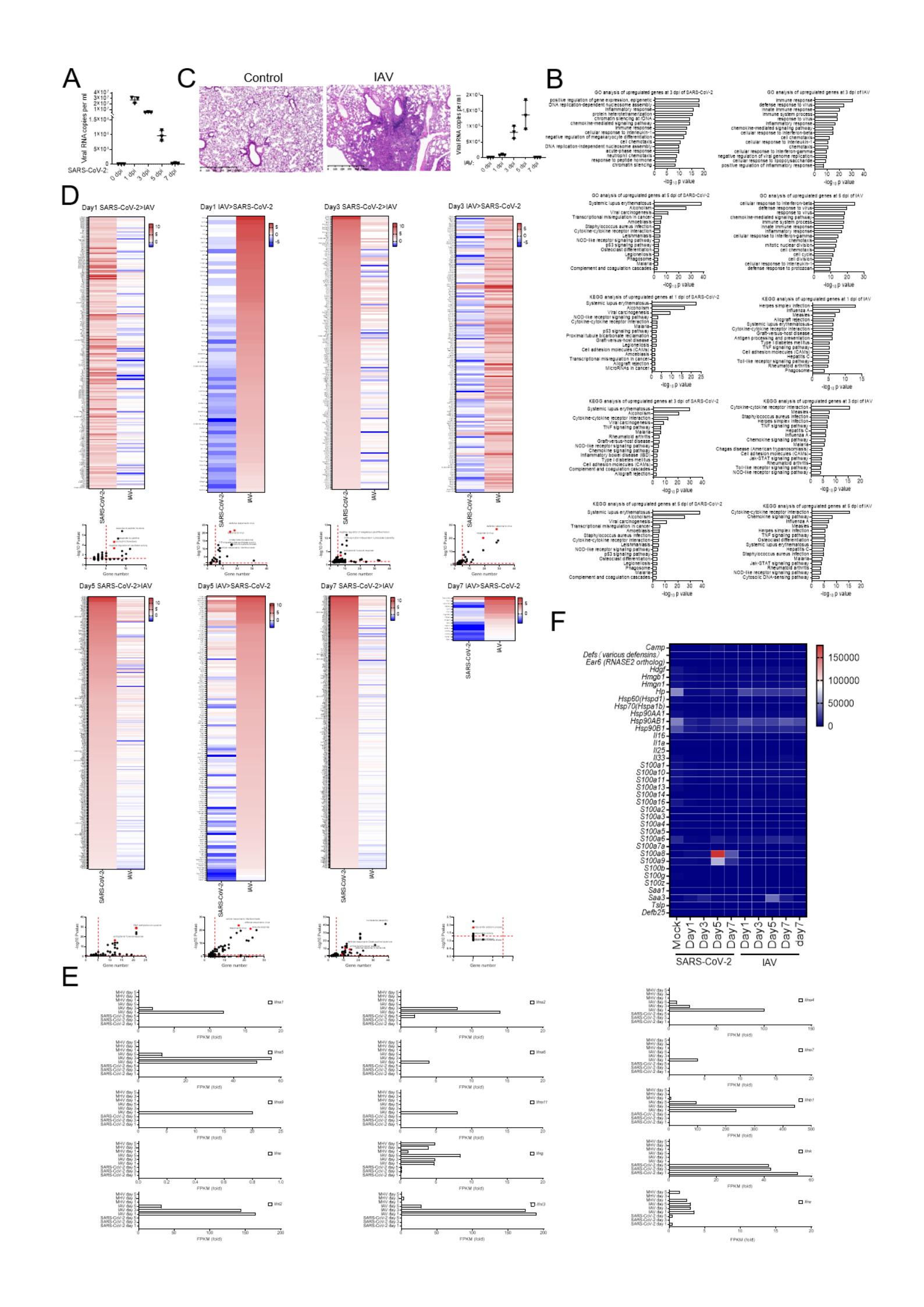
A
Viral RNA copies per ml
SARS-CoV-2:
0 dpi
1 dpi
3 dpi
5 dpi
7 dpi
C
Control
IAV
Viral RNA copies per ml
IAV:
B
GO analysis of upregulated genes at 3 dpi of SARS-CoV-2
GO analysis of upregulated genes at 3 dpi of IAV
GO analysis of upregulated genes at 5 dpi of SARS-CoV-2
GO analysis of upregulated genes at 5 dpi of IAV
KEGG analysis of upregulated genes at 1 dpi of SARS-CoV-2
KEGG analysis of upregulated genes at 1 dpi of IAV
KEGG analysis of upregulated genes at 3 dpi of SARS-CoV-2
KEGG analysis of upregulated genes at 3 dpi of IAV
KEGG analysis of upregulated genes at 5 dpi of SARS-CoV-2
KEGG analysis of upregulated genes at 5 dpi of IAV
-log10 p value
D
Day1 SARS-CoV-2>IAV
Day1 IAV>SARS-CoV-2
Day3 SARS-CoV-2>IAV
Day3 IAV>SARS-CoV-2
Day5 SARS-CoV-2>IAV
Day5 IAV>SARS-CoV-2
Day7 SARS-CoV-2>IAV
Day7 IAV>SARS-CoV-2
SARS-CoV-2
IAV
-log10 Pvalue
Gene number
F
Camp
Defs (various defensins)
Ear6 (RNASE2 ortholog)
Hdgf
Hmgb1
Hmgn1
Hp
Hsp60(Hspd1)
Hsp70(Hspa1b)
Hsp90AA1
Hsp90AB1
Hsp90B1
Il16
Il1a
Il25
Il33
S100a1
S100a10
S100a11
S100a13
S100a14
S100a16
S100a2
S100a3
S100a4
S100a5
S100a6
S100a7a
S100a8
S100a9
S100b
S100g
S100z
Saa1
Saa3
Tslp
Defb25
150000
100000
50000
0
Mock
Day1
Day3
Day5
Day7
Day1
Day3
Day5
Day7
day7
SARS-CoV-2
IAV
E
FPKM (fold)

Figure S2. Analysis of the differences between coronavirus and influenza a virus infection. (Related to Figure 2)

(A) qRT-PCR analysis for viral loads in the lungs of *hACE2* mice infected with SARS-CoV-2. *n=3*. **(B)** RNA-seq analysis of lungs in IAV- and SARS-CoV-2-infected mice at different points in time. GO and KEGG analysis were performed with the differentially expressed genes compared with Mock (*FC > 4 or < 0.25, P value < 0.05*). **(C)** Identification of a mouse model of pneumonia infected with IAV virus. H&E staining of the lung in mice infected with IAV at 5 dpi showed that lots of lymphocytes were infiltrating into the lungs and the lung tissue was obviously fibrotic. qRT-PCR analysis showed that IAV virus amplified effectively in the lung tissue. *n=3*. **(D)** GO and KEGG analysis was performed with the differentially expressed genes between IAV and SARS-CoV-2 infection (*FC > 4 or < 0.25, P value < 0.05*). **(E)** The expression of *IFNs* was analyzed by the RNA-seq data on lungs of mice infected by IAV, MHV or SARS-CoV-2. **(F)** Heat map depicting the expression of alarmins in the lungs of mice infected with IAV and SARS-CoV-2 at successive time points after infection.

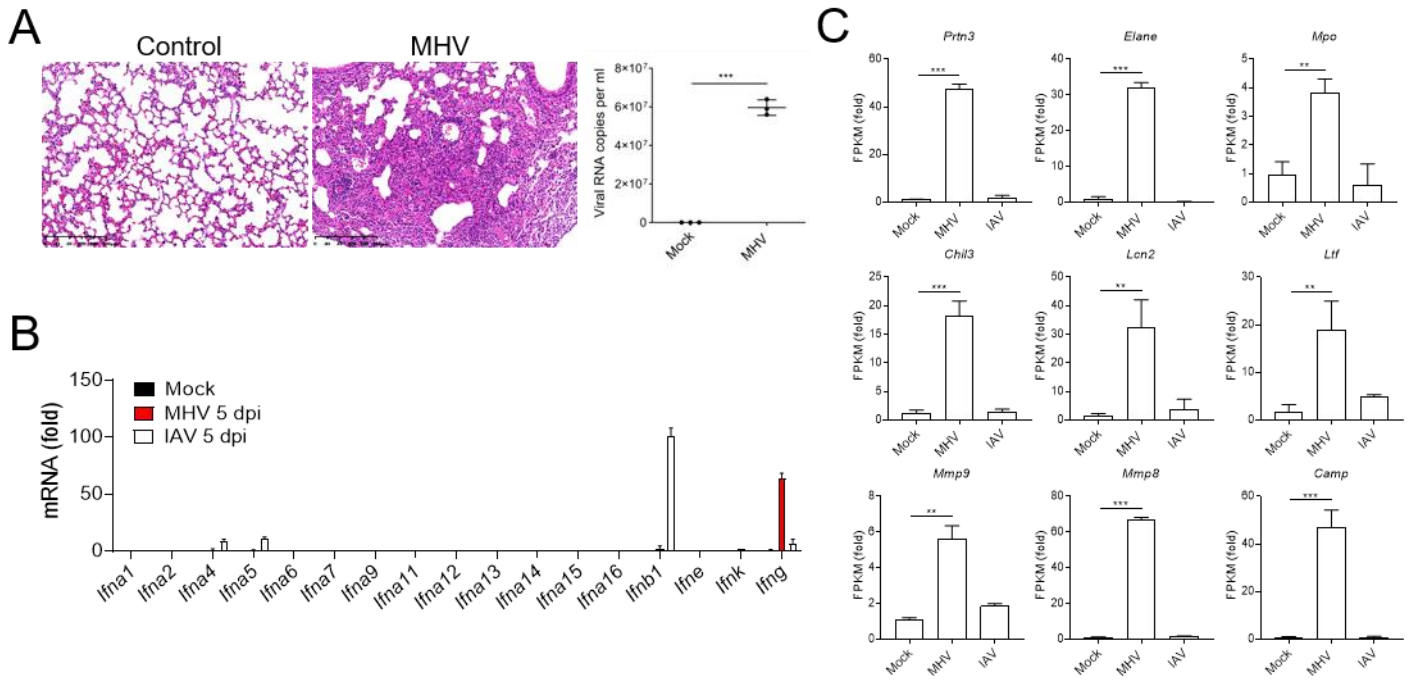

Figure S3. Analysis of immune characteristics of mouse coronavirus MHV-A59 infection. (Related to Figure 2).

(A) Identification of a mouse model of pneumonia infected with MHV virus. H&E staining of the lung in mice infected with MHV at 5 dpi showed significant pulmonary fibrosis. qRT-PCR analysis showed that MHV virus amplified significantly in the lung of mice. *n=3*. **(B)-(C)** The expression of *IFNs* (H) and neutrophil maker genes (I) in the lungs of mice infected with IAV or MHV at 5 dpi were analyzed using RNA-seq data (FC to Mock). (***P < 0.01; ***P < 0.001*).

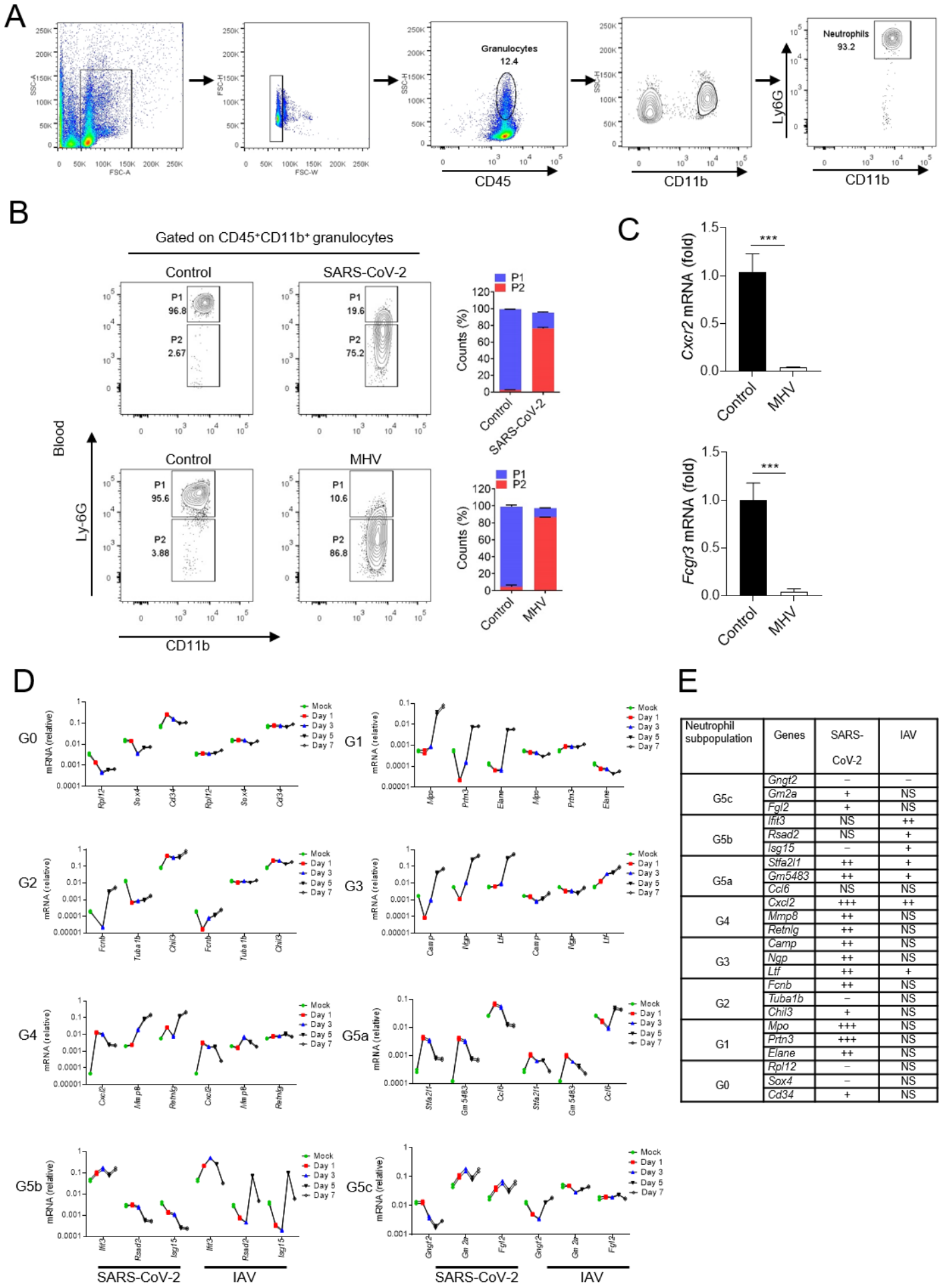

Neutrophil subpopulation	Genes	SARS-CoV-2	IAV
G5c	*Gngt2*	–	–
	Gm2a	+	NS
	Fgl2	+	NS
G5b	*Ifit3*	NS	++
	Rsad2	NS	+
	Isg15	–	+
G5a	*Stfa2l1*	++	+
	Gm5483	++	+
	Ccl6	NS	NS
G4	*Cxcl2*	+++	++
	Mmp8	++	NS
	Retnlg	++	NS
G3	*Camp*	++	NS
	Ngp	++	NS
	Ltf	++	+
G2	*Fcnb*	++	NS
	Tuba1b	–	NS
	Chil3	+	NS
G1	*Mpo*	+++	NS
	Prtn3	+++	NS
	Elane	++	NS
G0	*Rpl12*	–	NS
	Sox4	–	NS
	Cd34	+	NS

Figure S4. Aberrant neutrophils are closely associated with fatal coronavirus infection. (Related to Figure 3)

(A) A flow chart depicting the gating scheme of neutrophils. **(B)** Flow cytometry analysis of neutrophils in blood from mice infected with SARS-CoV-2 and MHV at 5 dpi. Gate P1 shows the conventional neutrophils ($CD45^{+}CD11b^{+}Ly6G^{high}$), and Gate P2 shows the pathologic aberrant neutrophils ($CD45^{+}CD11b^{+}Ly6G^{variable}$). Aberrant neutrophils (P2) in the blood of mice infected with coronavirus were significantly increased. $n = 3$. **(C)** qRT-PCR analysis for the expression of mature neutrophil marker genes *Fcgr3* and *Cxcr2* in aberrant neutrophils of bone marrow. $n = 3$. **(D)-(E)** RNA-seq analysis for related genes of neutrophil differentiation subgroup from the lungs of mice infected with SARS-CoV-2 or IAV. (***$P < 0.001$).

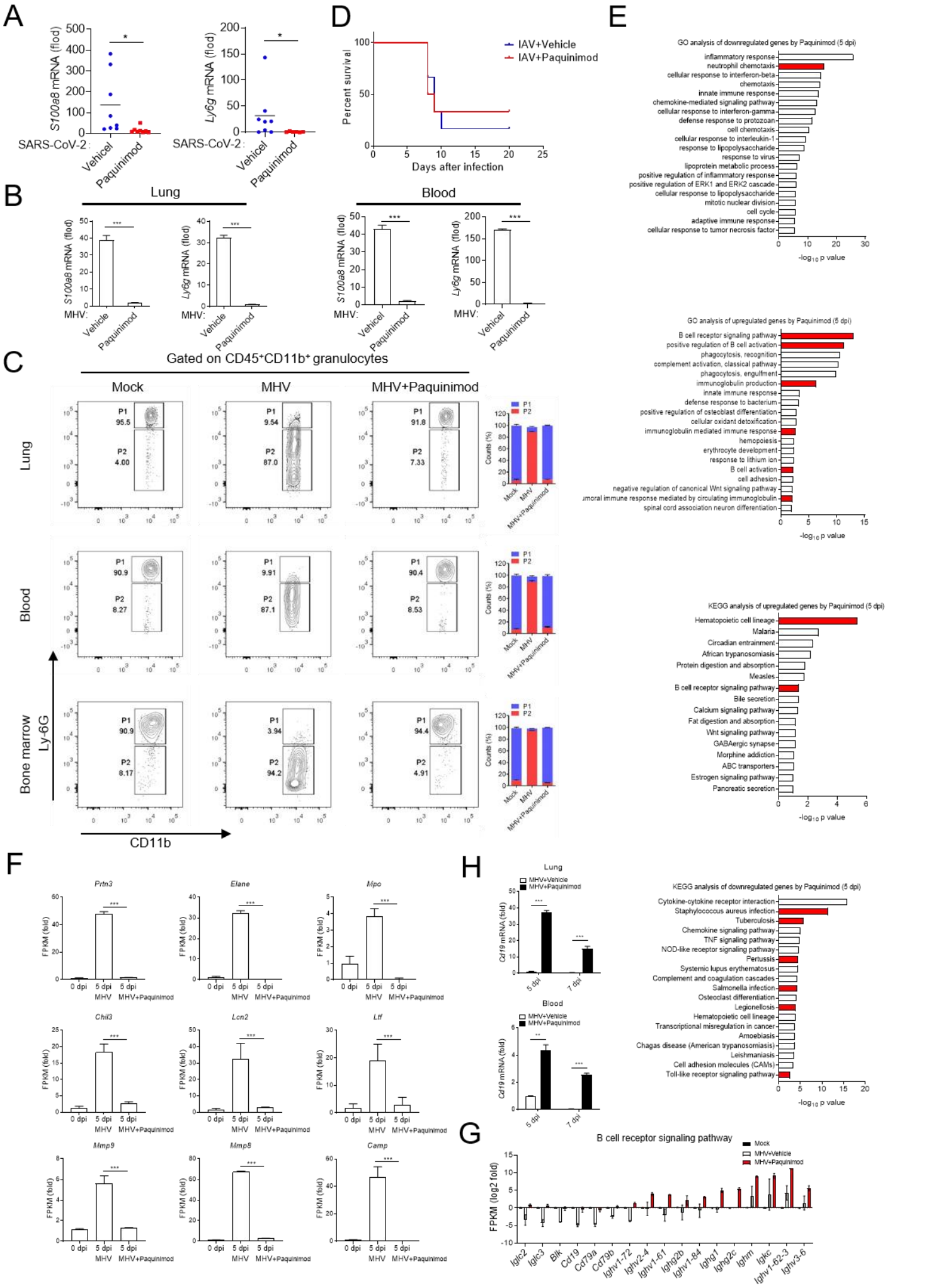
A
S100a8 mRNA (flod)
Ly6g mRNA (flod)
SARS-CoV-2 :
Vehicel
Paquinimod
D
Percent survival
Days after infection
IAV+Vehicle
IAV+Paquinimod
E
GO analysis of downregulated genes by Paquinimod (5 dpi)
inflammatory response
neutrophil chemotaxis
cellular response to interferon-beta
chemotaxis
innate immune response
chemokine-mediated signaling pathway
cellular response to interferon-gamma
defense response to protozoan
cell chemotaxis
cellular response to interleukin-1
response to lipopolysaccharide
response to virus
lipoprotein metabolic process
positive regulation of inflammatory response
positive regulation of ERK1 and ERK2 cascade
cellular response to lipopolysaccharide
mitotic nuclear division
cell cycle
adaptive immune response
cellular response to tumor necrosis factor
-log10 p value
B
Lung
Blood
MHV:
C
Gated on CD45+CD11b+ granulocytes
Mock
MHV
MHV+Paquinimod
Lung
Blood
Bone marrow
Ly-6G
CD11b
P1
P2
Counts (%)
GO analysis of upregulated genes by Paquinimod (5 dpi)
B cell receptor signaling pathway
positive regulation of B cell activation
phagocytosis, recognition
complement activation, classical pathway
phagocytosis, engulfment
immunoglobulin production
innate immune response
defense response to bacterium
positive regulation of osteoblast differentiation
cellular oxidant detoxification
immunoglobulin mediated immune response
hemopoiesis
erythrocyte development
response to lithium ion
B cell activation
cell adhesion
negative regulation of canonical Wnt signaling pathway
humoral immune response mediated by circulating immunoglobulin
spinal cord association neuron differentiation
KEGG analysis of upregulated genes by Paquinimod (5 dpi)
Hematopoietic cell lineage
Malaria
Circadian entrainment
African trypanosomiasis
Protein digestion and absorption
Measles
B cell receptor signaling pathway
Bile secretion
Calcium signaling pathway
Fat digestion and absorption
Wnt signaling pathway
GABAergic synapse
Morphine addiction
ABC transporters
Estrogen signaling pathway
Pancreatic secretion
F
Prtn3
Elane
Mpo
Chil3
Lcn2
Ltf
Mmp9
Mmp8
Camp
FPKM (fold)
0 dpi
5 dpi MHV
5 dpi MHV+Paquinimod
H
Lung
Blood
MHV+Vehicle
MHV+Paquinimod
Cd19 mRNA (fold)
5 dpi
7 dpi
KEGG analysis of downregulated genes by Paquinimod (5 dpi)
Cytokine-cytokine receptor interaction
Staphylococcus aureus infection
Tuberculosis
Chemokine signaling pathway
TNF signaling pathway
NOD-like receptor signaling pathway
Pertussis
Systemic lupus erythematosus
Complement and coagulation cascades
Salmonella infection
Osteoclast differentiation
Legionellosis
Hematopoietic cell lineage
Transcriptional misregulation in cancer
Amoebiasis
Chagas disease (American trypanosomiasis)
Leishmaniasis
Cell adhesion molecules (CAMs)
Toll-like receptor signaling pathway
G
B cell receptor signaling pathway
Mock
MHV+Vehicle
MHV+Paquinimod
FPKM (log2 fold)
Iglc2
Iglc3
Blk
Cd19
Cd79a
Cd79b
Ighv1-72
Ighv2-4
Ighv1-61
Ighg2b
Ighv1-84
Ighg1
Ighg2c
Ighm
Igkc
Ighv1-62-3
Ighv3-6

Figure S5. Analysis of the efficacy of Paquinimod in rescuing mice infected with coronavirus. (Related to Figure 4)

(A) qRT-PCR analysis for the expression of *S100a8* and *Ly6g* in the blood of mice infected with SARS-CoV-2 at 5 dpi after Paquinimod treatment. $n \geq 5$. **(B)** qRT-PCR analysis for the expression of *S100a8* and *Ly6g* in the lungs and blood of mice infected with MHV after Paquinimod treatment. $n = 3$. **(C)** Flow cytometry analysis of neutrophils in lungs, blood and bone marrow from mice infected with MHV at 5 dpi after Paquinimod treatment. Aberrant neutrophils (P2) in the mice infected with MHV were significantly decreased by Paquinimod treatment. $n = 3$. **(D)** Post-infection survival curves of wild type mice infected with IAV by Paquinimod treatment. $n=6$. **(E)** RNA-seq analysis for lungs of MHV-infected *Ifnar*$^{-/-}$ mice rescued by Paquinimod treatment at 5 dpi. GO and KEGG analysis was performed with the differentially expressed genes compared with control ($FC > 4$ *or* < 0.25, *P value* < 0.05). Control group means MHV-infected *Ifnar*$^{-/-}$ mice treated with Vehicle. **(F)** The expression of neutrophil maker genes in the lungs of MHV-infected mice rescued by Paquinimod at 5 dpi were analyzed by RNA-seq data. **(G)-(H)** Analysis of the expression level of B cell related genes in the lungs and blood of MHV-infected mice rescued by Paquinimod. $n = 3$. (*$P < 0.05$; **$P < 0.01$; ***$P < 0.001$).

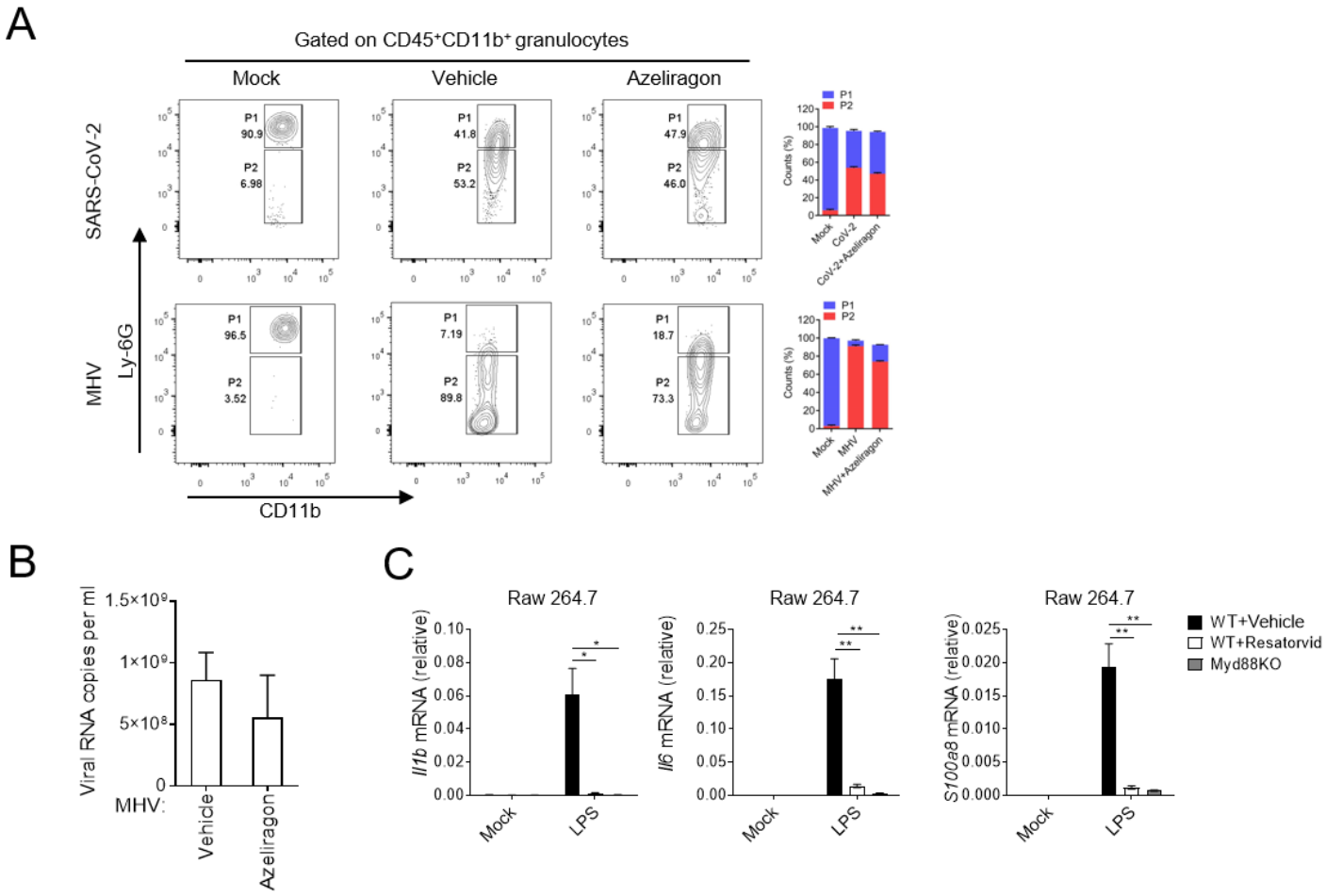

Figure S6. An attempt to treat mice infected with coronavirus via Azeliragon. (Related to Figure 5)

(A) Flow cytometry analysis of neutrophils in the lungs from mice infected with SARS-CoV-2 and MHV at 5 dpi after Azeliragon treatment. *n = 3.* **(B)** Analysis of viral loads in the lungs from MHV-infected mice at 5 dpi after Azeliragon treatment. *n = 3.* **(C)** Identified TLR4 signal response in the Raw 264.7 cells by qRT-PCR. *n = 3.* (*$P < 0.05$; **$P < 0.01$).